Lab on a Chip

Cite this: *Lab Chip*, 2011, **11**, 2385

www.rsc.org/loc

PAPER

A microfluidic platform for high-sensitivity, real-time drug screening on *C. elegans* and parasitic nematodes†

John A. Carr,[a] Archana Parashar,[a] Richard Gibson,[a] Alan P. Robertson,[b] Richard J. Martin[b] and Santosh Pandey*[a]

Received 28th February 2011, Accepted 3rd May 2011
DOI: 10.1039/c1lc20170k

This paper describes a new microfluidic platform for screening drugs and their dose response on the locomotion behavior of free living nematodes and parasitic nematodes. The system offers a higher sensitivity drug screening chip which employs a combination of existing and newly developed methods. Real-time observation of the entire drug application process (*i.e.* the innate pre-exposure locomotion, the transient response during drug exposure and the time-resolved, post-exposure behavior) at a single worm resolution is made possible. The chip enables the monitoring of four nematode parameters (number of worms responsive, number of worms leaving the drug well, average worm velocity and time until unresponsiveness). Each parameter generates an inherently different dose response; allowing for a higher resolution when screening for resistance. We expect this worm chip could be used as a robust cross species, cross drug platform. Existing nematode motility and migration assays do not offer this level of sophistication. The device comprises two principal components: behavioral microchannels to study nematode motility and a drug well for administering the dose and observing drug effects as a function of exposure time. The drug screening experiment can be described by three main steps: (i) 'pre-exposure study' – worms are inserted into the behavioral channels and their locomotion is characterized, (ii) 'dose exposure' – worms are guided from the behavioral microchannels into the drug well and held for a predefined time, during which time their transient response to the dose is characterized and (iii) 'post-exposure study' – worms are guided back into the behavioral microchannels where their locomotion (*i.e.* their time-resolved response to the dose) is characterized and compared to pre-exposure motility. The direction of nematodes' movement is reliably controlled by the application of an electric field within a defined range. Control experiments (*e.g.* in the absence of any drug) confirm that the applied electric fields do not affect the worms' motility or viability. We demonstrate the workability of the microfluidic platform on free living *Caenorhabditis elegans* (wild-type N2 and levamisole resistant ZZ15 *lev-8*) and parasitic *Oesophagotomum dentatum* (levamisole-sensitive, SENS and levamisole-resistant, LEVR) using levamisole (a well-studied anthelmintic) as the test drug. The proposed scheme of drug screening on a microfluidic device is expected to significantly improve the resolution, sensitivity and data throughput of *in vivo* testing, while offering new details on the transient and time-resolved exposure effects of new and existing anthelmintics.

Introduction

Many nematodes are ubiquitous soil-dwelling organisms and crucial for maintaining soil nutrients and overall symbiotic relationships between plants and other organisms.[1–3] However, numerous of the over 10,000 known nematode species are parasitic, infecting plants (*e.g.* corn, soybean, wheat, and other food grains), animals (*e.g.* pigs, sheep, goats, and cows) and humans.[1–3] The parasitic nematode of particular interest to this research, *Oesophagotomum dentatum* (*O. dentatum*), is a hog parasite that causes nodule growths in the pig's gut wall. These nodules repress growth and thereby reduce available pork yield. In this study, *O. dentatum* was chosen as a model for gut dwelling parasites. Conventional control methods based on chemotherapy face a major challenge as nematodes are developing drug resistance to the known anthelmintics.[1] Molecular mechanisms for detecting altered genotype due to drug resistance are time-consuming and do not easily translate to observable changes in phenotype.[1,4] Currently, a lack of information on the genomes of

[a]*Department of Electrical and Computer Engineering, Iowa State University, Ames, IA, 50011, U.S.A. E-mail: pandey@iastate.edu; Fax: +515.294.3637; Tel: +515.294.2740*
[b]*Department of Biomedical Sciences, Iowa State University, Ames, IA, 50011, U.S.A*
† Electronic supplementary information (ESI) available. See DOI: 10.1039/c1lc20170k

parasitic nematodes and physiological changes that occur with drug resistance has prevented the development of successful molecular biology assays. Thus, detection for drug resistance is classically observed using a fecal egg count reduction test followed by characterization on other assays such as migration inhibition assays,[5] larval development assay[6,7] or egg hatch assays.[8] Most anthelmintics tested in these assays (*e.g.* levamisole, monepantel, ivermectin, and piperazine) act on the nematode's neuromuscular system.[9] The limitations of the current technology and the development of resistant strains has brought forward the need for fast and reliable screening of existing and new anthelmintics.[1–3]

Popular present-day nematode motility assays (*e.g.* larval migration assay[5]) are based on a mesh system in which the worms resistant to a certain anthelmintic are able to move through the mesh, whereas the sensitive worms are restricted. A simple worm count gives the percentage of worms that were inhibited by the applied drug. Even though these assays are fairly simple and give a relatively good representation of worm survivability, they lack the throughput of information content needed to adequately test one or a range of anthelmintics.[5] Specifically, there are five main drawbacks to these motility assays. First, measurements are conducted on a worm population (50–100 samples) as it is difficult to evaluate a single nematode. Second, only one output parameter is monitored (*e.g.* percentage of worm survivability or inhibition), reducing the assays sensitivity and adaptability cross species and/or cross drug. Third, real-time observation of the drugs' transient effects is not possible as most methods rely on pre-treating the nematodes before observing them in the assay. Thus, locomotion behavior during this period is not fully known. Real-time observation of transient drug-effects has been previously displayed;[10] however, this device is not microscale. Hence, a higher volume of reagent is used, it is more expensive and difficult to fabricate (*e.g.* 3 acrylic plates were perforated with ninety-six holes using a laser precision system) and only a single parameter was monitored (*i.e.* worm activity).[10] Fourth, the monitoring of worm locomotion prior to exposure is not incorporated on-chip and, therefore, a direct comparison of the pre- and post-exposure behavior on the same population is not easily completed. Lastly, the total time for a single experiment is at least 4–6 h for even a trained experimentalist.[8,9] These drawbacks limit the design scope and flexibility of present day motility assays. As an alternative to motility assays, electrophysiological experiments conducted on the non-parasitic model nematode, *Caenorhabditis elegans* (*C. elegans*),[11–25] with specific ion-channels as drug targets provide valuable information about drug interactions at the molecular and cellular level but are labor-intensive and with low throughput.[9]

Recent advances in microfluidics have led to a new class of devices (culture and detection chambers,[26–28] cylindrical posts,[12] mazes,[29] piezoresistive sensors,[30] microtraps,[31,32] optofluidic microscopes,[33] clamp arrays[34] and olfactory chips[35]) to study the neurophysiology and behavior of nematode species. Microfluidics technology provides the potential advantage of conducting numerous experiments in parallel on the same chip with less reagents, improved sensitivity and increased resolution.[26,27] This, along with much improved imaging systems and automated data processing, has enabled the observation and characterization of key behavioral parameters *in vivo* at a micro- and nanoscale resolution. This has also inspired researchers to develop better quantitative models to describe phenotypic differences in nematodes under realistic environmental conditions.[35–40] In a related work on the application of microfluidics to parasitology, we fabricated straight microchannels and showed that their average velocity, oscillation frequency and body parameters (*i.e.* amplitude and wavelength) can be significantly different for levamisole-sensitive and levamisole-resistant strains of *O. dentatum*, even in the absence of the anthelmintic.[40] Building upon these results, we were able to develop a microfluidic drug screening chip that is not only capable of addressing the aforementioned drawbacks of present day motility assays, but can also help to correlate any change in phenotype associated with resistance.

In this paper, we present a new **H**igh-**S**ensitivity, **R**eal-**T**ime (HSRT) worm chip (Fig. 1a) for screening the drug resistance of *C. elegans* and parasitic nematodes. Our platform offers key advantages over our previous work[40] and other existing motility assays.[5] Specifically, a multi-parameter microfluidic bioassay has been developed to observe the innate locomotion of nematodes along with their transient and time-resolved responses to the application of anthelmintics (*i.e.* real-time observation from pre-exposure, through the drug exposure and to post-exposure) in a single experiment. Electrotaxis has been employed here as a reliable means to guide the movement of nematodes into and out of the drug well. Video recording of the entire experiment, along with an automated worm tracking software, revealed important information about changes in the worms' locomotion during the entry, exposure and exit periods. This information helped us develop multiple dose response curves and identify characteristics of drug resistance. Previously reported worm tracking programs were designed for studying *C. elegans* locomotion on agarose plates or sorting immobilized *C. elegans* mutants in microchannels based on phenotypic observations.[41–44] Our tracking software has the added advantage of autonomously measuring subtle locomotion changes in both *C. elegans* and other nematode species in microfluidic devices in the presence or absence of drugs. Besides quantifying transient drug effects, we were able to record and measure a number of locomotion parameters: (i) percentage of worms responsive, (ii) percentage of worms leaving the drug well, (iii) average post-exposure velocity and (iv) time until unresponsiveness. As we demonstrate later, this extraction of multiple parameters greatly improves the experimental sensitivity and the assay's adaptability to different species and drugs. We also reduced the experimental time for a single run (from 4–6 h[8,9] to ~60 min + the desired exposure time) and developed a parallel testing device that is chiefly limited by the microscope's field of view and the camera's resolution.

In order to realize a reliable drug screening platform independent of nematode species and test drug, several experimental aspects needed to be investigated. First, previous works[45–48] on the electrotactic response of nematodes were reproduced, extending them to the parasitic *O. dentatum* in the 'electrotaxis preference experiment'. Second, we characterized nematode behavior under different conditions of electric field and current in the 'electrotaxis sensitivity experiment'. Next, a method for selectively filling the microfluidic device was developed in order to create and maintain chemical separation without sacrificing electrical continuity across the device. Lastly, the proof-of-

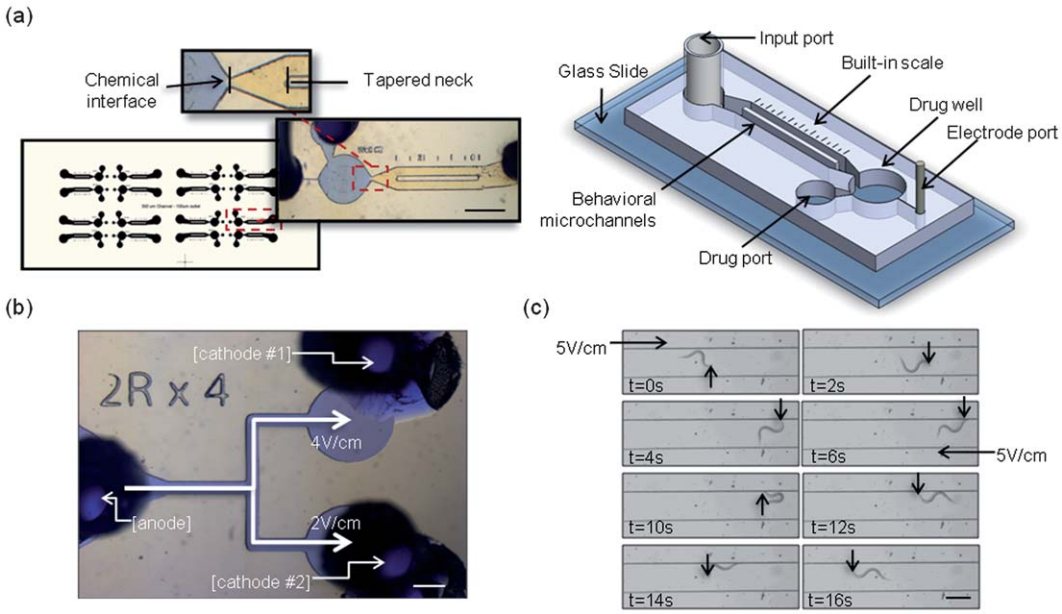

Fig. 1 The microfluidic devices used in this study. (a) [scale bar = 1.5 mm] Snapshot of the fabricated HSRT drug screening device comprising two microchannels tapering into a drug well. For illustration purpose, the two chemically separated agarose mixtures are colored with yellow and blue dyes. The soft-lithography mask is shown to illustrate the parallelism of the design. A 3D model showing the main components of the microfluidic design is also shown for further clarity. (b) [scale bar = 750 μm] Snapshot of the fabricated T-shaped microfluidic device showing the three electrode ports and sample electric fields at the respective ports. Worms are inserted in the left port and their preference to move towards either cathode is tracked with the imaging unit. (c) [scale bar = 300 μm] Time-lapsed images of a LEVR *O. dentatum* nematode in the straight microchannel. The position of the worm's head is indicated by an arrow. Initially, a 5 V cm^{-1} electric field directed to the right side is applied for a period of 6 s. The worm moves along the direction of the electric field. Thereafter, the direction of the electric field is reversed. The worm turns its body around at the 12th second and continues in the new direction of the electric field.

concept workability of the HSRT bioassay was shown by studying the multi-parameter dose response and transient exposure effects of levamisole on free-living *C. elegans* (wild-type and levamisole resistant, *lev-8*) and parasitic *O. dentatum* (levamisole-sensitive, SENS and levamisole-resistant, LEVR).

Experimental design

Experimental setup

The sample preparation described next, as well as the data analysis presented in the following section, is common for all experiments. The subsequent sections discuss each individual experiment in more detail.

All microfluidic chips were fabricated using a standard soft-lithography process. After fabrication, the PDMS chip was mechanically secured to the stage of a stereo microscope. Agarose (Fisher Scientific, Pittsburgh, USA), a linear polymer that when dissolved in water can be maintained as a liquid (>35 °C) or as a gel (<35 °C), was mixed at 0.8% w/v with tap water for *O. dentatum* experiments and M9 buffer for *C. elegans* experiments. The mixture was heated to 90 °C and magnetically stirred for 20 min. A small plastic tube was then connected to a syringe and the microfluidic device was filled with the liquid agarose mixture through the input ports. The agarose was subsequently allowed to cool and gelatinize into a porous gel through which the worms were able to move. To maintain a consistent viscosity, the experimental setup was maintained at ~25 °C. Nematode suspension was centrifuged to ~2 worms/μL and dropped into the input port(s). After a small scouting time (~5 min) the worms were able to penetrate into the agarose gel and populate the end of the channel(s) near the input port(s). A triple output power supply (HP/Agilent E3630A) was then connected to the chip's electrode ports by 1 cm long platinum electrodes. Using electrotaxis (field strength dependent upon the particular experiment), the nematodes were guided into the microchannels and their locomotion was recorded.

In order to observe and record the nematodes' motility, we used a Leica MZ16 transmission stereomicroscope. The microscope has a 1× and 2× objective lens, enabling 7.1× to 230× magnification which was adequate for the designed experiments. The microscope was coupled with a QICam 12-bit Mono Fast 1394 cooled digital camera interfacing with QCapture PRO software. This enables the capture of digital images (1392 × 1040 pixels) at a specified time interval (typically one second). The images from a recorded experiment were sequenced together and compressed into the Audio Video Interleave (.avi) video format.

Data analysis

The .avi video was then post-processed by our worm tracking program which extracts track signatures and locomotion parameters of individual worms. The source code was written in the C++ programming language. The program records and analyzes a large number of images (typically ~1200) to extract motility parameters such as amplitude, wavelength, forward velocity, path (*i.e.* track) traversed by the worm, track length,

number of halts and number of full reversals. The entire body of the nematode is represented by an articulated model composed of 13 connected segments approximating the worm's current posture. The centroid of the worm's body is tracked as it moves forward. In addition, the program provides track signatures of multiple nematodes simultaneously and is independent of the shape of the worm and whether the worms were confined in a single or multiple channels. The program is also adaptable to a range of image-capture speeds and image resolutions. The worm tracking program allows the user to adjust the resolution and zoom level such that there was less than a 1% error in worm length caused by rounding to the nearest pixel. The output of the worm-tracking software is a Microsoft Excel workbook containing a spreadsheet for each of the outputs requested by the user. A typical post-processing output file would include the following for every tracked worm: sequential x,y position coordinates, instantaneous velocity at each position, number of halts and reversals, and instantaneous locomotion amplitude and wavelength. GraphPad's prism (GraphPad, San Diego, USA) was then used to analyze and fit the generated data.

Design of the electrotaxis preference experiment

A key element towards developing the microfluidic drug screening platform was the use of an electrical field to direct the worms throughout the device. Electrotaxis of *C. elegans* has been shown on agarose plates and in microscale chambers where the worms tend to migrate towards the cathode.[45–48] Switching the direction of the electric field switched the direction of the *C. elegans*' movement. Published work on electrotactically-guided nematode movement shows that the electrosensory behavior has a neural basis in *C. elegans*.[46] It has been proposed that the *C. elegans* electrosensory behavior may have evolved as a strategy for nematode parasites (cousins of the *C. elegans*) to exploit directional cues inside their host.[46] Therefore, it can be reasonably hypothesized that any nematode possessing such amphid sensory neurons will exhibit some electrotaxis. However, variability in electrotaxis (*e.g.* electric field range) between *C. elegans* strains has been reported.[46,47] Thus, open questions remained as to the exact electrotactic response of the *O. dentatum* species.

To demonstrate electrotaxis on the parasitic nematode species studied here, we characterized the preference of the worm to a range of different electric fields. T-shaped microfluidic devices were fabricated (width = 300 μm, length = 1 cm, height = 40 μm) (Fig. 1b). Each device consisted of three input ports connected *via* straight microchannels. The nematodes were placed in the left port and voltages were applied to establish two uniform electric fields. The anode (left port) was biased at 0V and the cathodes (right ports) were biased at two different negative voltages. The worms were free to move in the microchannels, their progression was recorded and a data set containing number of worms collected at each cathode was obtained.

Design of the sensitivity to the applied electric field experiment

To further quantify the currently published threshold and maximum applicable fields (3 V cm^{-1} and 14V cm^{-1} respectively for *C.* elegans[46]), we next investigated the ideal range of electric field for guiding the parasitic nematodes throughout the microfluidic device without adversely damaging their natural sinusoidal movement. This range of electric field was investigated in two steps. First, by sweeping the cathode voltage at a high (>10 MΩ) microchannel resistance, a minimum electric field was found at which the direction of the nematodes movement could be reliably controlled. Second, by varying the microchannel resistance at a fixed cathode voltage (~4.5 V), a maximum allowable current was found beyond which the nematodes become unresponsive (*i.e.* cease movement). This value of current was used to infer the maximum allowable electric field for a given microchannel resistance.

The test for electrotaxis sensitivity was performed on straight microchannels (width = 300 μm, length = 1 cm, height = 40 μm) (Fig. 1c). Similar to the procedure in the abovementioned T-shaped devices, the nematodes were placed into the input ports and a uniform electrical field was established. To find the minimum electric field, the anode was kept at 0V while the cathode was biased at certain negative voltage (−1.0 V to −5.0 V) to sweep the electric field strength within the device. The anode and cathode were interchanged once every minute, hence, switching the direction of the electric field. The worms' progression was recorded and a data set containing the number of worms responding (*i.e.* changing the direction of their forward movement) to the switch in field direction was obtained. To find the maximum allowable current, the voltage at the cathode was fixed (4.5 V) and the electrical resistance of the device was varied (2 MΩ to 11 MΩ) by altering the length of the microchannel (a channel resistance *vs.* channel length graph is provided in the ESI, 'SF1 _Resistance *vs.* Channel length'†) to sweep the electric current strength within the device. External, series connected axial lead resistors were used to help control the maximum current and to keep the electric field over the channel relatively consistent between ~3.5 and ~4.5 V cm^{-1}. As before, the direction of electric field was switched every minute and a data set of the number of worms responding was obtained.

Design of the high-speed, real-time screening of drug resistance experiment

Our HSRT device, depicted in Fig. 1a, consists of two behavioral microchannels (width = 300 μm; length = 1 cm; height = 80 μm for *C. elegans* and height = 40 μm for *O. dentatum*), a drug well (radius = 850 μm), an input port (radius = 900 μm), a drug port (radius = 900 μm) and an electrode port (radius = 600 μm; connected to the drug well *via* a 750 × 15 μm channel). The drug well is connected to the behavioral microchannels by a tapered neck (length = 750 μm, starting width = 700 μm and ending width = 200 μm). Two parallel microchannels were chosen in order to keep the number of worms per channel at a level that allowed accurate data analysis (*i.e.* to avoid aggregation where a single worm was not distinguishable) while keeping the total sample count high. The worms were first inserted into the microchannels through the input port and their innate pre-exposure locomotion (*e.g.* average forward velocity) was characterized. The worms were then guided into the drug well where they were held for a predefined exposure time. During this period, the transient effects of the drug on locomotion were characterized at real-time. Lastly, the worms were guided back into the microchannels where post-exposure locomotion was

characterized and compared to pre-exposure locomotion to determine the time-resolved effects of the drug.

Developing on our previous work,[40] it was the primary goal of this research to fabricate a robust worm chip with the ability to screen drug resistance at a higher sensitivity, to allow a direct comparison of innate behavior to time-resolved drug response behavior and to quantify the nematode's transient response during the exposure period. To help accomplish this, we developed a unique two-step method for filling the device to virtually limit the drug within the drug well. In order to maintain a surface profile that restricted fluidic flow and allowed for better control while filling the device with the agarose solution, we found a treatment of the PDMS surfaces to be crucial. Although hydrophobic by nature (contact angle ~90–120°), it is known that plasma oxidized PDMS exhibits hydrophilic properties (contact angle ~5–60°) for as long as 6 days after treatment (up to 2 weeks for full recovery).[49–51] Therefore, the HRST device was filled with a octadecyltrichlorosilane (OTS) solution (OTS: n-hexadecane = 2 : 100 v/v) and left to dry at room temperature for ~2 h. The OTS treatment coated the entire device with a thin, hydrophobic film; providing better control of the flow profile. This allowed us to selectively fill the behavioral microchannels/tapered neck with an agarose/buffer mixture and subsequently fill the drug well with agarose/buffer/drug mixture. The two-step filling process enabled us to chemically separate the drug well from the behavioral microchannels and yet maintain electrical conductivity throughout the device. Supplementary electrokinetic experiments (incorporating diffusion, electro-osmotic and electrophoretic effects) using Fluorescein dye (MW = 322 g) demonstrate a majority of the drug-well (>93%) is kept within 5% of the desired concentration during the entire course of the HSRT bioassay experiments (with no noticeable gradient within the well). Further, the experiments revealed any diffusion (at concentrations up to 100 μM Fluorescein) is contained within the 1,000 μm tapered neck – which acts as a spacer between the drug well (having ~100% of the dose) and behavioral microchannels (having ~0% of the dose). Our experiments show the concentration decays through the neck very quickly (100 μM dose in well has an average half-length = 360 μm; 30 μM dose in well has an average half-length = 270 μm; both half-lengths are ≤ length of an *O. dentatum* nematode). As an example, we found a worst case scenario (100 μM Fluorescein through a 45 min experiment) reached the end of its decay near the interface of the tapered neck and behavioral channels. Using an average nematode's forward velocity (120–140 μm s^{-1} as we will later show) this worst case condition represents an increase of only ~14.14 s or ~1.8% (accounting for both input and output through the tapered neck) in exposure time. ESI file 'SF3 _Diffusion and Electrokinetics. pdf' contains further information on the drug well/behavioral channel isolation.†

After filling the microfluidic device, nematode suspension was placed on the input port and worms were allowed to enter into the microchannels. The anode, biased at 0 V, was placed in the input port and the cathode, biased at −5 V, was placed in the electrode port. A uniform electric field was established, thereby directing a finite number (~1 to ~25, determined by the density of suspension) of worms through the behavioral channel into the drug well. The worms' progression was recorded and a data set of pre-exposure motility (*i.e.* velocity, wavelength, amplitude and track signature) was obtained. The electric field was kept for a defined exposure time (15 min was used for levamisole testing; exposure times of up to ~1 h were successfully tested) which held the worms in the drug well and ensured that they received maximum exposure to the drug. A data set of worm motility, namely the time until worm inhibition during the exposure time, was obtained. Subsequently, the direction of the electric field was reversed and the uninhibited worms were guided from the drug well into the microchannels. The worms' progression was again recorded and a data set of post-exposure motility was obtained. A comparison between pre-exposed and post-exposed worm parameters (average velocity of worms in microchannel, number of worms entering/leaving drug well, number of worms responsive in the device and time until drug has taken full effect) provided information about the dose response and were used to identify resistant isolates or mutants.

Results and discussions

Preference to negative electric field

Fig. 2a plots the preference of SENS and LEVR *O. dentatum* nematodes when choosing between a pair of electric field strengths in the T-shaped microchannels. The data presented in the four bar graphs (Fig. 2a i–iv) shows that a high percentage (>80%) of the *O. dentatum* nematodes prefer to travel towards the cathode having the lower potential. For example, in Fig. 2a ii, more than 89% (n = 49, SENS and n = 68, LEVR) of the two *O. dentatum* isolates chose to travel to the cathode kept at an electric field of 4 V cm^{-1} while less than 10.5% of the nematodes move to the cathode kept at 2 V cm^{-1}. Furthermore, Fig. 2a i suggests that, when given an option between a floating cathode (which has no electric field) and a cathode kept at a finite electric field (4 V cm^{-1}), the nematodes chose the path of nonzero electric field. This shows that nematodes prefer to move in the path of the field lines rather than seeking an escape route out of the area of field application. As seen from all the graphs (Fig. 2a i–iv), there is no significant difference (P value > 0.05) between SENS and LEVR isolates in their direction of preference. In accordance with current literature,[44–47] our observations on L4 stage *C. elegans* show that they also prefer to move towards the more negative cathode. Hence, the application of electric field could be used as a reliable means of guiding nematodes into and out of different sections of our microfluidic device.

Characterizing electrotaxis sensitivity

In Fig. 2b we plot the sensitivity of SENS and LEVR *O. dentatum* nematodes to electric field strength measured in straight microchannels. In both figures (Fig. 2b i,ii), the raw data is fitted using a Boltzmann sigmoidal function. As shown in Fig. 2b i (in the absence of levamisole), a low percentage (< 10%) of SENS and LEVR isolates respond to field strengths below 2 V cm^{-1}. A higher percentage of worms start responding with increasing field strength; the percentage rise is sharper for LEVR isolate (45% increase for a 0.25 V cm^{-1} change) compared to that for the SENS (25% increase for a 0.25 V cm^{-1} change). The maximum percentage of worms responding to the electric field reached 89% at 5 V cm^{-1} (n = 202) for LEVR while it reached 79% (n = 100) for SENS. An F test was used to compare top saturation regions

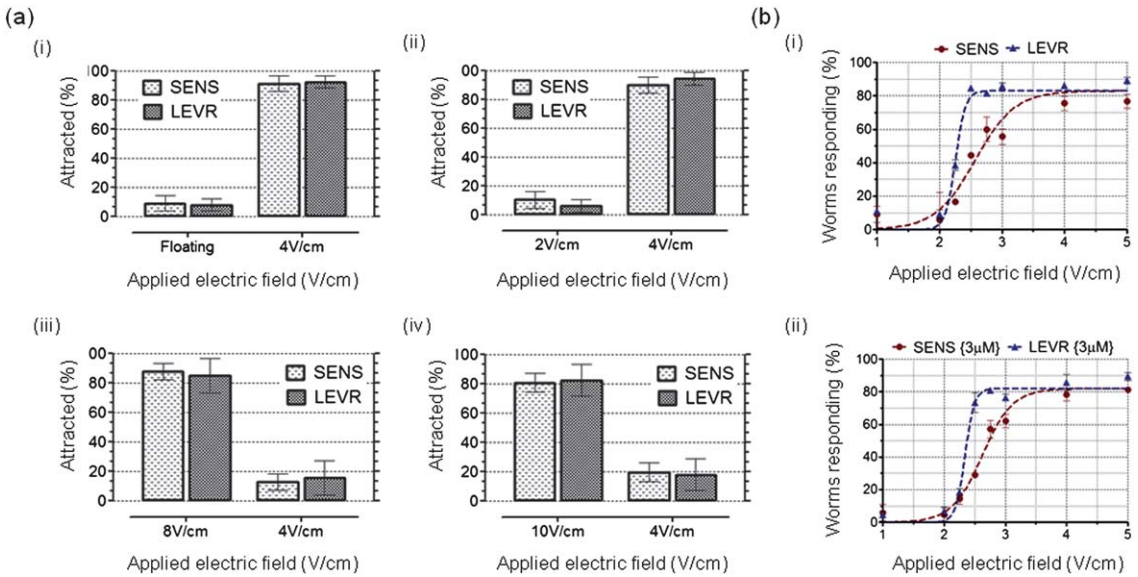

Fig. 2 Electrotaxis preference and sensitivity results for *O. dentatum* nematodes (a) The preference data for SENS and LEVR nematodes between four pairs of electric fields is shown (i–iv). The percentage of the total *O. dentatum* nematodes attracted by each electric field is plotted. (b) The sensitivity data for SENS and LEVR nematodes in the absence and presence of 3 μM levamisole. The percentage of worms responding to the applied electric field is plotted. In the absence of levamisole (i), few worms (< 10%) are responsive below electric fields of 2 V cm^{-1} while most worms (83% LEVR, 83% SENS) respond to electric fields above 4 V cm^{-1}. Exposure to 3 μM levamisole does not significantly alter the worms' responsiveness to the electric field (ii).

of the two sigmoidal fits: the global comparison revealed a preferred model of equivalent tops for both fits (F value (DFn, DFd) = 2.94 (1, 10), P value = 0.12). This shows that no significant statistical distinction can be made between the electrotactic responses of SENS and LEVR above an applied field of 4 V cm^{-1}. It was the goal of this experiment to determine the minimum electric field strength to induce an equivalent response in both isolates; hence, 4.5 V cm^{-1} was chosen for use in the HSRT bioassay. In another set of experiments, to ensure that electrotaxis could be used in combination with drug exposure, the *O. dentatum* nematodes were pre-treated (~1 h) with 3 μM levamisole and their electrotaxis sensitivity was again characterized. Fig. 2b ii shows that 3 μM levamisole does not significantly alter the electrotaxis sensitivity plots from Fig. 2b i – especially above 4 V cm^{-1} (SENS: F value (DFn, DFd) = 0.85 (3, 10), P value = 0.49; LEVR: F value (DFn, DFd) = 2.79 (3, 10), P value = 0.10). Thus, we were able to conclude that a field in the range of 4.5 V cm^{-1} was a suitable control field for *O. dentatum* in the presence and absence of the drug. In both experiments we have closely matched the threshold field of current literature (~3 V cm^{-1}[47]) and offered further information on the subthreshold behavior and differences between the two *O. dentatum* isolates. In accordance with current works, our observations on L4 *C. elegans* show that an operating field in the range of 6.5 V cm^{-1} was suitable for controlling their movement.[47]

Fig. 3a i shows the response of a representative LEVR nematode upon applying a 4.5 V cm^{-1} electric field to a microchannel with an electrical resistance of ~12 MΩ (current in channel = ~0.37 μA). Here, the worm was initially travelling to the left side. Upon turning the field on, the worm retracts, turns its head around and the rest of the body follows. Eventually, the worm moves to the right side in the direction of the applied field. Fig. 3a ii shows the response of a LEVR nematode upon applying a ~4.5 V cm^{-1} electric field to a microchannel with an electrical resistance of ~2 MΩ (current in channel = ~1.80 μA). Here, the worm was initially travelling to the left side. Upon turning the field on, the worm does retract but fails to take a directional cue from the applied field and, thus, control is lost. We observed many worms curled (as in Fig. 3a ii) when subjected to this higher current, but this curling was only temporary and the worms' random exploration typically ensued after this short break.

Fig. 3b plots the sensitivity of SENS and LEVR *O. dentatum* nematodes to the current flowing in the microchannel. The percentage of worms responding as a function of the channel resistance is shown (~3.5–4.5 V cm^{-1} applied). Previous work shows *C. elegans* quickly paralyze in fields stronger than 14 V cm^{-1}.[46] Further, this work showed that, by varying the salt concentration (*i.e.* the conductivity) of agar surfaces, the effects of increased current were negligible on the electrotactic response of the worms.[46] In contrast, our work on *O. dentatum* found that as the channel current was increased, directional control over a majority of nematode population within the device was lost. In conjunction with the data provided in Fig. 2b, a majority of nematodes (>83% responding; n = 30, SENS and n = 36, LEVR) could be controlled (*i.e.* exhibited an electrotactic response) at a channel resistance greater than 11 MΩ; which corresponds to a channel current of less than 0.4 μA. Above a channel current of 1.5 μA (~2.5 MΩ), however, most control (≤20% responding; n = 28, SENS and n = 58, LEVR) of the *O. dentatum* nematodes was lost. Following these results, we chose a channel resistance of at least 10MΩ in our later drug screening experiments to ensure a strong electrotactic response of both isolates.

To test whether motility parameters were affected by the electric field, our automated worm-tracking software was used to measure the average forward velocity of SENS and LEVR *O. dentatum* nematodes under different electric fields (see the ESI file 'SF4 _Sample tracking data' for a sample track output†). A

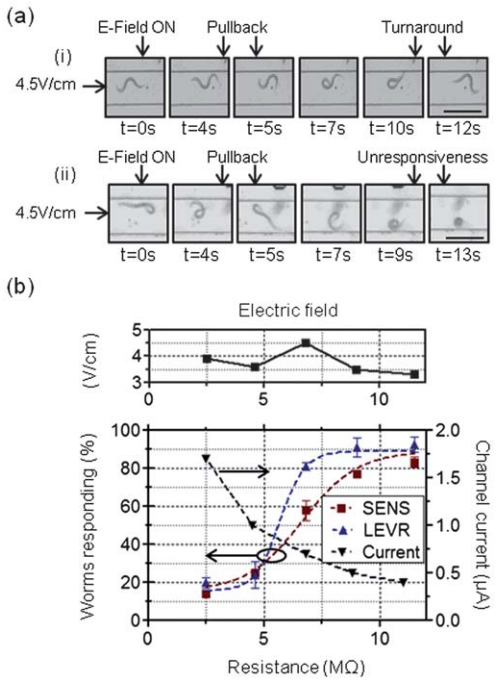

Fig. 3 Effects of decreasing channel resistance and characterization of nematode velocity in an electric field. (a) [scale bar = 300 μm] Time-lapsed images of a LEVR *O. dentatum* nematode in the straight microchannel are shown for a low (~0.3 μA) (i) and high (~2.5 μA) (ii) current in the channel. The electric field is turned on at time t = 0 and the reaction of the worm is videographed. In the case of low current, the worm initially retracts, turns its head around to align with the field direction and begins to move in the direction of the electric field. In the case of high current, the worm initially retracts, but quickly curls and becomes unresponsive. (b) The effect of changing the net resistance of the microchannel on the *O. dentatum* nematodes. As the resistance is decreased, the current flowing in the microchannel increases. At currents above 1 μA, more worms are hindered by the current and become unresponsive – thus control of worm movement is lost.

post-processing script was then used to calculate the average velocity of any extended, uninhibited forward movement (*i.e.* a span of movement where the worm moves for >500 μm without touching another worm or a channel wall). As seen in Fig. 4 (n = 20–80), the forward velocity is unchanged under various field strengths (143 ± 2 μm s^{-1} for LEVR and 123 ± 2 μm s^{-1} for SENS). When pre-treated with 3 μM levamisole, the respective velocities decrease (132 ± 3 μm s^{-1} for LEVR and 88 ± 2 μm s^{-1} for SENS) due to the drug's effects but remain relatively unchanged under different electric fields. The measured velocity data in the presence of an electric field closely correlates with our previous results on *O. dentatum* in straight microchannels.[40] This result is in accordance with recent work that shows *C. elegans'* velocity remains unaltered within different electric field strengths.[47]

Real-time screening of drug resistance

Levamisole was chosen as the pilot drug for our proof-of-concept study to show the workability of the HSRT worm chip as its dose response is well-characterized and it serves as a good standard to

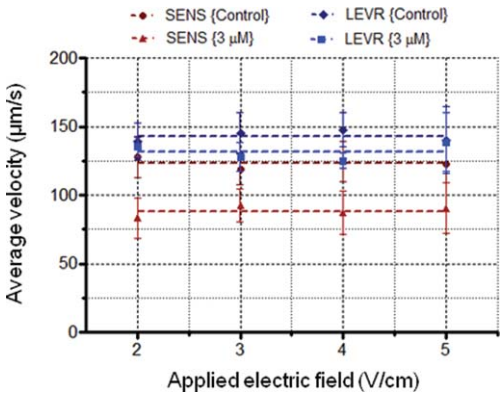

Fig. 4 The measured velocity of the worms' centroid position is plotted at different electric fields. The average velocity is unaffected by the applied electric field and confirms that the electric field only influences the direction of movement. These results are in correlation with previously published results on *C. elegans*.[47]

assess the performance of our new platform. From the experiments, we extracted four dose response parameters: (i) percentage of worms responsive, (ii) percentage of worms leaving the drug well, (iii) average post-exposure velocity and (iv) time until unresponsiveness. Each parameter inherently produces a different dose response and is a different measure of drug resistance.

Fig. 5a i,ii (n = 20–105) show the percentage of responsive worms (parameter (i)) as a function of levamisole dose for *O. dentatum* and *C. elegans* respectively. Here, we defined responsiveness as the ratio of the worms able to move outside a defined circular area to the total number of worms in the device. A circle, with a radius equal to the worm's body length, is drawn around the worm. Once the worm's movement is completely contained within this circle it is concluded that the worm is inhibited such that it cannot move any significant distance. Fig. 5b shows a visual representation of tracking data (generated by our worm tracking software) for a single N2 *C. elegans* exposed to a 100 μM dose in the drug well. The figure shows that, as time progresses, the overall surface area covered by the worm's movement reduces. The worm is defined as unresponsive when this area becomes smaller than the area of a circle with a radius equal to the worm's body length. Using GraphPad Prism software, the data was fitted using a Response *vs.* log(Dose) curve. To ensure the best fit for both data sets, the *O. dentatum* model constrained the Hill slope to a value of 1.0 and the *C. elegans* model allowed the Hill slope to vary. These models allowed us to determine the EC_{50} values, defined as the concentration that provokes a response half way between the basal and maximal response, of the agonist (levamisole) and compare for differences between isolates or strains. Table 1 summarizes the EC_{50} generated by parameter (i). Dose response parameter (i) closely resembles the inhibition parameter measured in traditional worm motility assays. For comparison, the EC_{50} values for levamisole on the survivability assay were found to be 15 μM for SENS, 40 μM for LEVR, 9 μM for N2 and 40 μM for *lev-8*. Fig. 6a i,ii shows the percentage of worms leaving the drug well (parameter (ii)) as a function of levamisole dose for *O. dentatum* and *C. elegans* respectively. The EC_{50} values produced by parameter (ii) are

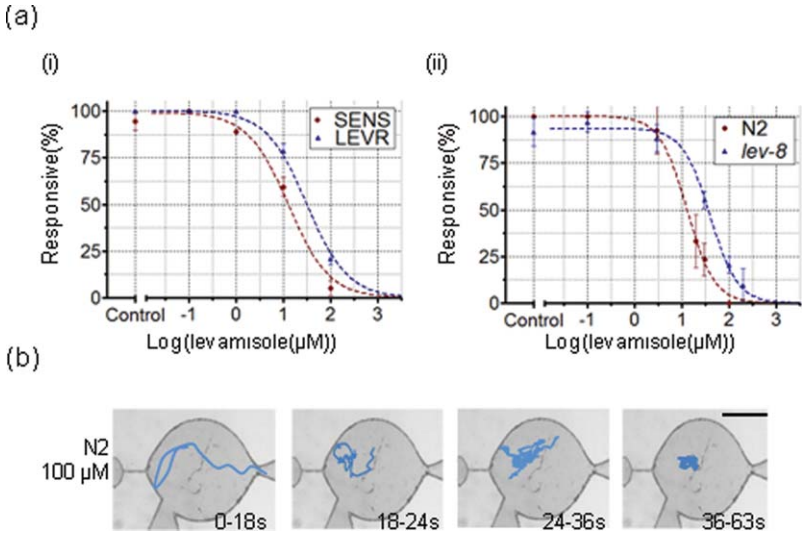

Fig. 5 (a) Dose response generated by parameter (i), percentage of worms responsive, for *O. dentatum* (SENS and LEVR) (i) and *C. elegans* (L4 stage N2 and *lev-8*) (ii) nematodes in the microfluidic drug screening device. At low levamisole concentrations (0.1 μM for SENS, 10 μM for LEVR, 1 μM for N2 and 3 μM for *lev-8*), almost all worms are responsive. At higher concentrations, the percentage of worms unresponsive increases and eventually, at the cutoff concentration (~100 μM for SENS, ~150 μM for LEVR, ~100 μM for N2 and ~250 μM for *lev-8*), all worms are unresponsive. (b) [scale bar = 0.5mm] Representative tracks of L4 stage N2 *C. elegans* in the drug well of the microfluidic drug screening device. The tracks, shown as a function of time, give quantification as to how movement changes when the worm exposed to high (100 μm) dose of the drug. Initially, worm movement is spread over a large surface area; as time progresses, the amount of surface area reduces and eventually the worm becomes unresponsive.

shown in Table 1. Fig. 6b i,ii shows average worm velocity (parameter (iii)) as a function of levamisole dose for *O. dentatum* and *C. elegans* respectively. Both pre- and post-exposure velocities are plotted to further highlight the effect of the drug. Our assay is advantageous as both pre- and post-exposure velocities can be directly monitored. Thus, a normalized velocity (post-exposure divided by pre-exposure velocity) can be calculated and small inconsistencies between experiments (*e.g.* room temperature) are removed. The normalized graphs and EC_{50} values are provided as ESI ('SF2 _Normalized velocity graphs').† Table 1 presents the EC_{50} values determined by parameter (ii).

Table 2 summarizes the EC_{50} ratios of LEVR to SENS and *lev-8* to N2. This ratio can be used to check how pronounced the drug resistance (if any) between two isolates or strains is; a higher ratio is representative of a larger difference in EC_{50} and a more pronounced drug resistance. An F test was used to determine if the EC_{50} values of two isolates or strains are significantly different. For each species, the smallest P value (*i.e.* the most statistically significant difference) is displayed in blue, while any parameters not representative of resistance are shown in red. The table highlights that, in single-parameter platforms, sensitivity may be lost as the assay is adapted to new species and drugs. In other words, the monitored parameter may be the best for species X (e.g *C. elegans*) but not for species Y (*e.g. O. dentatum*). For example, parameter (i) (worms responsive) showed the best measurement of resistance for the *C. elegans* strains studied here, but parameter (ii) (worms leaving) (and, as we will later see, parameter (iv): time until unresponsiveness) was shown to be the best for *O. dentatum.* Parameter (iii) (worm velocity) exhibited no resistance for the *C. elegans* strains but was the 2nd best measure for *O. dentatum.* Further, the monitored parameter of current assays may be a good measure for a drug that affects overall responsiveness or inhibition but may not be adequate for a toxin that only affects a particular aspect of locomotion (*e.g.* velocity). This issue is better addressed in our platform as the multi-parameter monitoring is made possible by the novel design. For further comparison, the survivability assay produced ratios of 2.7 (LEVR/SENS) and 4.5 (*lev-8*/N2). Both of which are smaller than the ratios generated by the HSRT's parameter (ii) (worms leaving). This indicates that the worm chip presented here is of higher resolution and allows us to detect more subtle phenotypic changes associated with drug resistance compared to survivability assays.

Fig. 7a plots the transient response of the drug effect (parameter (iv)) on the nematodes for a dose of 100 μM levamisole. The sample minimum, lower quartile, median, upper

Table 1 Summary of levamisole EC_{50} values generated by the HSRT bioassay

	Worms Responsive		Worms Leaving		Worm Velocity	
	EC_{50}	Log(EC_{50} (μM))	EC_{50}	Log(EC_{50} (μM))	EC_{50}	Log(EC_{50} (μM))
SENS	13 μM	1.11 ± 0.11	2 μM	0.36 ± 0.07	2 μM	0.38 ± 0.16
LEVR	32 μM	1.50 ± 0.07	12 μM	1.07 ± 0.09	12 μM	1.09 ± 0.08
N2	13 μM	1.11 ± 0.05	10 μM	1.05 ± 0.10	22 μM	1.34 ± 0.04
lev-8	40 μM	1.60 ± 0.04	47 μM	1.67 ± 0.07	29 μM	1.46 ± 0.06

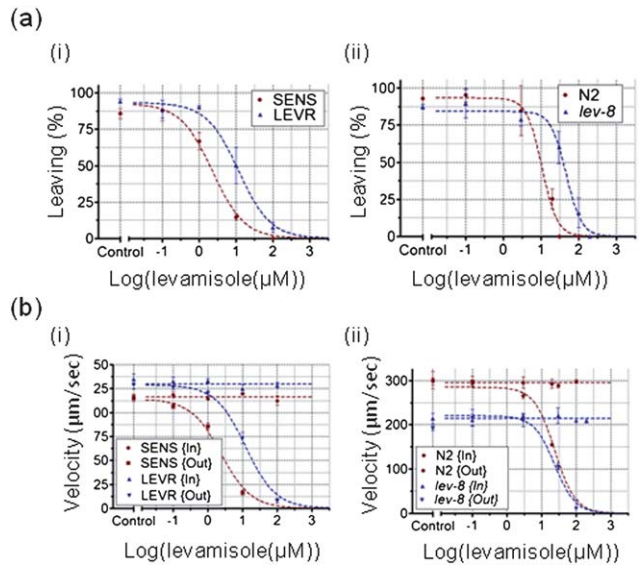

Fig. 6 (a) Dose response parameter (ii), percentage of worms leaving the drug well to the total worms entered, is plotted for *C. elegans* (i) and *O. dentatum* (ii). Below a certain concentration (0.1 μM for SENS, 1.0 μM for LEVR, 0.1 μM for N2 and 0.1 μM for *lev-8*), most of the worms (>90%) entering the drug well are able to exit after exposure. Above this concentration, the percentage of worms that manage to exit the drug well decreases steadily. Above a cutoff concentration (100 μM for SENS, 150 μM for LEVR, 30 μM for N2 and 150 μM for *lev-8*), all worms are unable to exit the drug well. (b) Dose response parameter (iii), average velocity, is plotted for *C. elegans* (i) and *O. dentatum* (ii). At concentrations higher than 0.1 μM, the SENS velocity decreases sharply while the LEVR velocity exhibits a sharp decrease above 1.0 μM (a-i). For *C. elegans*, the N2 forward velocity decreases sharply at concentrations higher than 1.0 μM, while the *lev-8* velocity shows a similar decrease above 3 μM (a-ii).

quartile and sample maximum of the total time from exposure to unresponsiveness for both *O. dentatum* and *C. elegans* are displayed. As shown, the drug effect is established (*i.e.* the test nematode is inhibited such that it cannot move outside a circle with a radius equal to its body length) in SENS (median = 3.7 min; n = 17) sooner than in LEVR (median = 8.5 min; n = 14) and much earlier in N2 (median = 0.4 min; n = 14) compared to *lev-8* (median = 3.8 min; n = 11) mutant. This highlights that our drug screening device offers a unique advantage of monitoring the transient effects of drug exposure with the ability to characterize the locomotion parameters at a single worm resolution.

Fig. 7b shows time lapsed images of a single SENS nematode being exposed to a 100 μM dose of levamisole in the drug well. For the initial few minutes, there were no observable changes in the worm's sinusoidal movement. Within the next 2–5 min, we observed that the worm gradually curled up and was eventually paralyzed. The time response for observing drug effects can be used as a fourth parameter for characterizing drug resistance. In a two-tailed, nonparametric t-test with Welch's correction, a comparison of the LEVR/SENS medians revealed a difference of 4.68 min and a P value = 0.0016. This represents a significant difference ($P < 0.05$) between the isolates, indicating a levamisole resistance and a pronounced phenotypic change in the LEVR isolate. In the same test, a comparison of the *lev-8*/N2 medians revealed a difference of 1.73 min and a P value = 0.0007. Again, this represents a significant difference and is indicative of a levamisole resistance in the *lev-8* mutant. The result shows this parameter can be confidently used to screen resistance. Interestingly, parameter (iv) was the best statistical measure of resistance for *O. dentatum* and the second best measure for *C. elegans.*

Conclusion

In conclusion, we presented a new tool for screening anthelmintic drugs on both free living and parasitic nematodes. The proposed device offers a higher sensitivity, all-inclusive drug screening chip that is easily fabricated and uses a low volume of reagent. Real-time observation of the entire drug screening process (*i.e.* the innate pre-exposure locomotion, the transient response during drug exposure and the time-resolved, post-exposure behavior) at a single worm resolution is made possible. The chip enables the monitoring of four system parameters (*i.e.* average velocity, number of worms leaving the drug well, the number of active worms and time until unresponsiveness), which provides a higher resolution (*i.e.* lower EC_{50}, lower P values, and higher F values) when screening for resistance and allows for a robust cross species, cross drug platform. The experimental time for measuring dose response is considerably decreased from several hours for traditional worm motility assays to 40–60 min in our device. The workability of the HSRT bioassay was shown on the parasitic *O. dentatum* and the free living *C. elegans* with levamisole as the pilot drug. This demonstration of a non-black-box, more accurate, multi-parameter microfluidic drug screening device is expected to help future work on new and existing anthelmintics, their rapid screening and elucidation of underlying cellular/molecular interactions.

Table 2 Summary of levamisole EC_{50} ratios (LEVR to SENS; *lev-8* to N2) generated by the HSRT bioassay (most significant resistance measurements indicated in blue; non-significant resistance measurements indicated in red)

	Worms Responsive			Worms Leaving			Worm Velocity		
	EC_{50} ratio	F value (DFn, Dfd)	P value	EC_{50} ratio	F value (DFn, Dfd)	P value	EC_{50} ratio	F value (DFn, Dfd)	P value
LEVR/SENS	2.50	11.62 (1,4)	0.0271	**6.00**	**41.82 (1,4)**	**0.0029**	6.00	24.86 (1,3)	0.0155
***lev-8*/N2**	**3.10**	**70.51 (1,5)**	**0.0004**	4.70	40.38 (1,5)	0.0014	**1.30**	**1.46 (1,2)**	**0.3506**

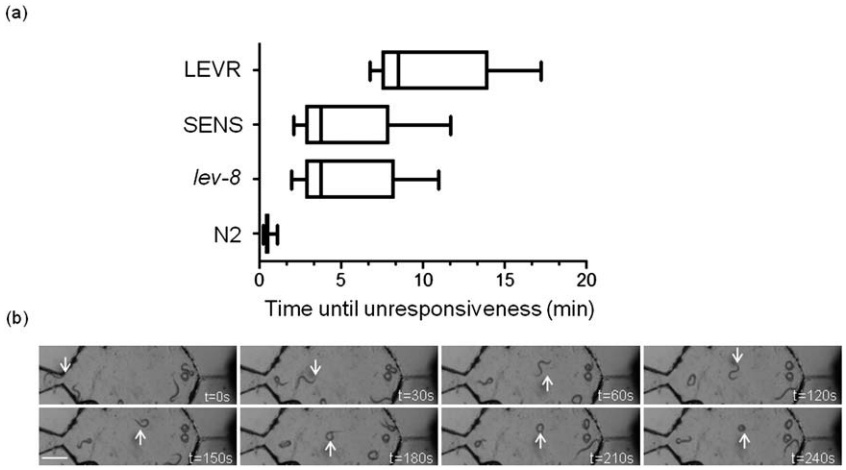

Fig. 7 Time response of the drug effect on the nematodes in the drug well. (a) Box plot of the total time from initial exposure of 100 μM levamisole to unresponsiveness for *O. dentatum* and L4 stage *C. elegans*. Median times for restraint strains (LEVR median = 8.5 min; *lev-8* median = 3.750 min) were found to be significantly higher than the median times of their sensitive counterparts (SENS median = 3.7 min; N2 median = 0.4 min). (b) [scale bar = ~200μm] Time-lapsed images of SENS *O. dentatum* being exposed to 100 μM levamisole in the drug well. The drug effect is tracked on a particular nematode (indicated with an arrow). The worm is able to move freely in the initial 120 s, after which time the drug begins to render the worm unresponsive within the next 120 s.

Experimental

Fabrication of PDMS devices

The fabrication was done using standard micromachining and soft lithography procedures.[53] The layout was drawn in AutoCAD and sent to an outside vendor (Fineline Imaging, Colorado Springs, CO) to generate the emulsion masks. A 40 μm or 80 μm thick negative tone photoresist (NANO™ SU-8 2-25; Microchem Corporation, Newton, MA) layer was cast onto a bare silicon wafer by spin coating (~2800 r.p.m; single spin technique for 40 μm layer; double spin technique for 80 μm). Photolithography was carried out to create the final SU-8 master mold. The PDMS prepolymer (Sylgard 184 Silicone Elastomer Kit, Dow Corning Corporation, Midland, MI) was cast over the SU-8 mold and cured on a hot plate at 70 °C for two hours. Subsequently, the PDMS microfluidic devices were peeled off the mold and input ports (2 mm diameter) were punched into the device. Air plasma was exposed to the PDMS devices, which were then bonded to individual glass coverslips.

Maintaining the nematodes

Levamisole-sensitive (SENS) and resistant (LEVR) *O. dentatum* were originally supplied by the Royal Veterinary and Agricultural School, Frederiksberg, Copenhagen and then reproduced at six to nine months interval by passage in pigs at Iowa State University, Ames, Iowa. The L3 larvae isolates were maintained between passages in tap water refrigerated at 11 °C (changed every 2–4 months). Wild-type (N2) and *lev-8* (*ZZ15*) mutant *C. elegans* were obtained from the Caenorhabditis Genetics Center (CGC) at University of Minnesota (St. Paul, USA). The *C. elegans* were cultivated at 25 °C on Nematode Growth Medium (NGM) plates seeded with *Escherichia coli* OP50 bacteria. For our experiments, L4 stage *C. elegans* were picked using a sterilized platinum wire.

M9 buffer recipe

The recipe used for the M9 buffer (3 g KH_2PO_4, 6 g Na_2HPO_4, 5 g NaCl, 1 ml 1 M $MgSO_4$, H_2O to 1 liter) is a standard recipe taken from the Wormbook.

Worm tracking program

The worm tracking program ran the recorded worm videos through a number of steps to negate the background and extract worm motility parameters.

Background negation was performed first. This step was used to negate the channel walls, other markings, and any particulates. It was able to identify the background in the presence of many worms by comparing a series of images over the duration of the input video. As the worms moved, they exposed new parts of the background. For each successive image, areas that were lighter than previous frames were added to the background model. Combining a number of frames in this way produced a complete background model. The background was negated and a threshold was applied. This produced an output video containing only white worms on an empty black background.

The Lucas-Kanade optical flow algorithm was used to compute motion vectors. Worm density and movement did not affect the tracking system. It only used vectors that agree across the whole view, ignoring localized movements caused by worms. The algorithm generated motion vectors by tracking image features of the worm which may also have included particulates on the substrate or other unwanted patterns incorporated during channel fabrication. To characterize motion in any direction, the program detected features in the image which have both sharp vertical and horizontal components. It also compensated for vibrations that occurred during the recording procedure by using the image-feature tracking technique.

In addition, the user was able to easily provide the program with information about regions of interest. This specified the

areas of the video that should be processed further, ignoring the rest. This allowed the user to safely ignore irrelevant data, shorten execution time, and use separate sets of data from parallel experiments running in different channels.

The next step was worm segmentation and recognition. After background subtraction, polygons were fitted to the white shapes. Isolated regions such as particulates that do not have an interior area were eliminated, leaving only the channel boundaries. This step was used to improve performance and accuracy by safely ignoring erroneous data outside the channels and also to segregate data from multiple channels. Polygons that were too large or too small were discarded. This included instances where two or more worms were in contact. Worm polygons were then matched between consecutive frames to provide tracking data over time. If no close match was found in the next frame, which may occur because of worm occlusion or worm contact, the track was terminated. If the same worm was recognized in later frames, a new track was started.

The last step was the extraction of motility parameters. The centroid of the worm at each frame was calculated as the centroid of the fitted polygon. The polygon was also used to calculate the bounding box to approximate the wavelength and amplitude. The posture of the worm was represented by a series of segments running along its center. The program first found a pair of points across the middle of the worm. The points were then alternately advanced (first in one direction and then the other) to minimize the distance between the points until they met at the end of the worm. For each successive position of the points, the midpoint was added to the worm's spline. The spline points were then simplified to thirteen equally spaced points. We then extracted the track signatures from the gathered data.

Evolution of the 2-step filling process

Our initial attempts involved filling the entire microchannel and drug well with a drug/buffer/agarose mixture. The worms were then placed in the input port and guided into the drug well. While accomplishing the goal of both transient and time-resolved locomotion characterization, this method limited our ability to quantify pre-exposure locomotion parameters as the worms were exposed to the drug even in the microchannels. Our second attempt relied on a diffusion method in which we filled the mirochannels and drug well with a buffer/agarose mix and then allowed the drug to diffuse into the drug well *via* the drug inlet. Although this method enabled real-time characterization and allowed us to monitor pre-exposure locomotion parameters, the rate of drug diffusion was difficult to control and the dose present in the drug well could not be accurately calibrated. In our third and successful attempt, we developed a method of filling the two sections (microchannels and drug well) of the device with two chemically-different (agarose/buffer and agarose/buffer/drug) media in a two-step process.

Acknowledgements

The project was supported by Grant Number R 01 AI 047194 from the National Institute of Allergy and Infectious Diseases to RJM, an Iowa Center Neurotoxicology grant to APR and NSF-CMMI-1000808 grant from the National Science Foundation to SP and RJM. The content is solely the responsibility of the authors and does not necessarily represent the official views of the National Institute of Allergy and Infectious Diseases of the National Institutes of Health.

Notes and references

1 R. M. Kaplan, *Trends Parasitol.*, 2004, **20**, 477–481; K. R. Barker, R. S. Hussey, L. R. Krusberg, G. W. Bird, R. A. Dvnn, V. R. Ferris, D. W. Freckman, C. J. Gabriel, P. S. Grewal, A. E. Macguidwin, D. L. Riddle, P. A. Roberts and D. P. Schmitt, *J. Nematology*, 1994, **26**, 127–137.
2 M. Albonico, V. Wright, M. Ramsan, H. J. Haji, M. Taylor, L. Savioli and Q. Bickle, *Int. J. Parasitol.*, 2005, **35**, 803–811.
3 A. Diawara, L. J. Drake, R. R. Suswillo, J. Kihara and D. A. Bundy, *PLoS Neglected Trop. Dis.*, 2009, **3**, e397.
4 P. S. Dittrich and A. Manz, *Nat. Rev. Drug Discovery*, 2006, **5**, 210–218.
5 H. P. Tang, C. Ho and S. S. Lai, *Rapid Commun. Mass Spectrom.*, 2006, **20**, 2565–2572.
6 M. A. Taylor, K. R. Hunt and K. L. Goodyear, *Vet. Parasitol.*, 2002, **103**, 183–194.
7 E. O. Lind, A. Uggla, P. Waller and J. Höglund, *Vet. Parasitol.*, 2005, **128**, 261–269.
8 A. C. Kotze, S. Clifford, J. O'Grady, J. M. Behnke and J. S. McCarthy, *Am. J. Trop. Med. Hyg.*, 2004, **71**(5), 608–616.
9 R. J. Martin, *Vet. J.*, 1997, **154**, 11–34; R. J. Martin, G. Bai, C. L. Clark and A. L. Robertson, *Br. J. Pharmacol.*, 2003, **140**, 1068–1076.
10 S. H. Simonetta and D. A. Golombek, *J. Neurosci. Methods*, 2007, **161**, 273–280.
11 L. A. Herndon, P. J. Schmeissner, J. M. Dudaronek, P. A. Brown, K. M. Listner, Y. Sakano, M. C. Paupard, D. H. Hall and M. Driscoll, *Nature*, 2002, **419**, 808–814.
12 S. R. Lockery, K. J. Lawton, J. C. Doll, S. Faumont and S. M. Coulthard, *J. Neurophysiol.*, 2008, **99**, 3136–3143.
13 J. T. Pierce-Shimomura, T. M. Morse and S. R. Lockery, *J. Neurosci.*, 1999, **19**, 9557–9569.
14 J. M. Gray, D. S. Karow, H. Lu, A. J. Chang, J. S. Chang, R. E. Ellis, M. A. Marletta and C. I. Bargmann, *Nature*, 2004, **430**, 317–322.
15 J. M. Gray, J. J. Hill and C. I. Bargmann, *Proc. Natl. Acad. Sci. U. S. A.*, 2005, **102**, 3184–3191.
16 G. M. Whitesides, *Nature*, 2006, **442**, 368–373.
17 D. B. Weibel, P. Garstecki and G. M. Whitesides, *Curr. Opin. Neurobiol.*, 2005, **15**, 560–567.
18 K. Nahui, C. M. Dempsey, J. V. Zoval, J. Sze and M. J. Madou, *Sens. Actuators, B*, 2007, **122**, 511–518.
19 C. I. Bargmann and H. R. Horvitz, *Neuron*, 1991, **7**, 729–742.
20 S. H. Chalasani, N. Chronis, M. Tsunozaki, J. M. Gray, D. Ramot, M. B. Goodman and C. I. Bargmann, *Nature*, 2007, **450**, 63–70.
21 N. Chronis, M. Zimmer and C. I. Bargmann, *Nat. Methods*, 2007, **4**, 727–731.
22 T. Wakabayashi, I. Kitagawa and R. Shingai, *Neurosci. Res.*, 2004, **50**, 103–111.
23 R. D. Cole, G. L. Anderson and P. L. Williams, *Toxicol. Appl. Pharmacol.*, 2004, **194**, 248–256.
24 G. L. Anderson, W. A. Boyd and P. L. Williams, *Environ. Toxicol. Chem.*, 2001, **20**, 833–838.
25 R. J. Dobson, A. D. Donald, P. J. Waller and K. L. Snowdon, *Vet. Parasitol.*, 1986, **19**, 77–84.
26 N. Chronis, *Lab Chip*, 2010, **10**, 432–437.
27 D. B. Weibel, W. R. DiLuzio and G. M. Whitesides, *Nat. Rev. Microbiol.*, 2007, **5**, 209–218.
28 A. C. Miller, T. R. Thiele, S. Faumont, M. L. Moravec and S. R. Lockery, *J. Neurosci.*, 2005, **25**, 3369–3378.
29 J. Qin and A. R. Wheeler, *Lab Chip*, 2007, **7**, 186–192.
30 S. J. Park, M. B. Goodman and Beth L. Pruitt, *Proc. Natl. Acad. Sci. U. S. A.*, 2007, **104**, 17376.
31 C. B. Rohde, F. Zeng, R. Gonzalez-Rubio, M. Angel and M. F. Yanik, *Proc. Natl. Acad. Sci. U. S. A.*, 2007, **104**, 13891–13895.
32 K. Chung, M. M. Crane and H. Lu, *Nat. Methods*, 2008, **5**, 637–643.
33 X. Heng, D. Erickson, L. R. Baugh, Z. Yaqoob, P. W. Sternberg, D. Psaltis and C. Yang, *Lab Chip*, 2006, **6**, 1274–1276.

34 S. E. Hulme, S. Shevkoplyas, A. McGuigan, J. Apfeld, W. Fontana and G. M. Whitesides, *Lab Chip*, 2010, **10**, 589–597.
35 Y. Zhang, H. Lu and C. I. Bargmann, *Nature*, 2005, **438**, 179–184.
36 R. McNeal, Taylor and Francis, London, 2002, 345.
37 N. A. Croll, *Adv. Parasitol.*, **13**, 71–122; N. A. Croll, *J. Zool.*, 2009, **176**, 159–176.
38 E. Niebur and P. Erdos, *Math. Biosci.*, 1993, **118**, 51–82; E. Niebur and P. Erdos, *Biophys. J.*, 1991, **60**, 1132–1146.
39 C. J. Cronin, J. E. Mendel, S. Mukhtar, Y. M. Kim, R. C. Stirbl, J. Bruck and P. W. Sternberg, *BMC Genet.*, 2005, **6**, 5.
40 B. Chen, A. Deutmeyer, J. Carr, A. P. Robertson, R. J. Martin and S. Pandey, *Parasitology*, 2010, **138**, 80.
41 Z. Feng, C. J. Cronin, J. H. Wittig, P. W. Sternberg and W. R. Schafer, *BMC Bioinformatics*, 2004, **5**, 115.
42 W. Geng, P. Cosman, C. C. Berry, Z. Feng and W. R. Schafer, *IEEE Trans. Biomed. Eng.*, 2004, **51**, 1811–1820; J. H. Baek, P. Cosman, Z. Feng, J. Silver and W. R. Schafer, *J. Neurosci. Methods*, 2002, **118**, 9–21.
43 G. Tsibidi and N. Tavernarakis, *BMC Neurosci.*, 2007, **8**, 86.
44 D. Ramot, B. E. Johnson, T. L. Berry, L. Carnell and M. B. Goodman, *PLoS One*, 2008, **3**, e2208.
45 N. C. Sukul and N. A. Croll, *J. Nematol.*, 1978, **10**, 314–317.
46 C. V. Gabel, H. Gabel, D. Pavlichin, A. Kao, D. Clark and A. Samuel, *J. Neurosci.*, 2007, **27**, 7586–7596.
47 P. Rezai, A. Siddiqui, P. R. Selvaganapathy and B. P. Gupta, *Lab Chip*, 2010, **10**, 220–226.
48 P. Rezai, A. Siddiqui, P. R. Selvaganapathy and B. P. Gupta, *Appl. Phys. Lett.*, 2010, **96**, 153702–153703.
49 D. Bodas and C. Khan-Malek, *Sens. Actuators, B*, 2007, **123**, 368–373.
50 S. Gillmor, B. Larson, J. Braun, C. Mason, L. Cruz-Barba, F. Denes and M. Lagally, *Proceedings of the 2nd Annual IEEE-EMBS Special Topic Conference in Microtechnologies in Medicine and Biology*, Wisconson-Madison, USA, 2002.
51 S. Mata, A. J. Fleischman and S. Roy, *Biomed. Microdevices*, 2005, **7**, 281–293.